

Effects of Graphite Additions and Heat Treatment on the Microstructure, Mechanical and Tribological Properties of 13% Chromium White Iron

J. O. Agunsoye¹, S. A. Bello¹, I. O. Awe², A. A. Yekinni³, R. G. Adeyemo¹, A. O. Ologunagba¹

¹Department of Metallurgical and Materials Engineering, University of Lagos, Lagos, Nigeria

²Department of Metallurgical Engineering, Yaba College of Technology, Lagos, Nigeria

³Department of Mechanical Engineering, Lagos State Polytechnic, Ikorodu, Nigeria

Email: jagunsoye@unilag.edu.ng, adekunle_b@yahoo.com, kunleyk2003@yahoo.com

Received 27 March 2014; revised 2 May 2014; accepted 13 May 2014

Copyright © 2014 by authors and Scientific Research Publishing Inc.

This work is licensed under the Creative Commons Attribution International License (CC BY).

<http://creativecommons.org/licenses/by/4.0/>



Open Access

Abstract

A 13% chromium white iron was produced using a stir cast process. Samples of the produced white iron were austenised at 1450°C and then quenched in water to the room temperature. The characterisation tools such as X-ray diffractometer, scanning electron microscope, Brinell hardness tester and pin on disc machine were employed in the studies of the phase orientation and morphology, hardness value measurement and investigation of wear behaviour. The results revealed that water quenching the 13% chromium white iron led to the precipitation of fine iron chromides and cementite in the matrix of martensite. Moreover, there is an about 22% to 45% increase in hardness values of the as-cast 13% chromium white iron as the %composition of graphite additions increased from 1.36 to 3.04. However, the impact energy values are sacrificed. The increase in hardness values is attributable to hard intermetallic compounds such as iron chromides and cementite phases in the iron matrix. Also, there is an about 32% - 42% increase in hardness values of the heat treated samples of 13% chromium white iron when compared with those of the as-cast. The increased hardness values are attributable to even distribution of the fine intermetallic compounds in the fine grains of martensitic matrix. The wear rate increased as the sliding moments per unit time increased due to increasing work done by the friction to oppose the rotation of the pin on disc. The water quenched 13% chromium white iron samples have greater wear resistances than the as-cast samples due to their greater hardness values than those of the as-cast samples. The effect of speed increase on decreasing wear resistances is more pronounced on the heat treated samples than on the as-cast samples. Hence, the water quenched 13% chromium white iron is an excellent material in application requiring high wear resistance and low impact energy especially in grinding mill liner plate, bottom or casing used in the concrete pipe production, roller for crushing and pulverising mills.

How to cite this paper: Agunsoye, J.O., *et al.* (2014) Effects of Graphite Additions and Heat Treatment on the Microstructure, Mechanical and Tribological Properties of 13% Chromium White Iron. *Journal of Minerals and Materials Characterization and Engineering*, 2, 270-285. <http://dx.doi.org/10.4236/jmmce.2014.24032>

Keywords

13% Chromium White Iron, Water Quench, Microstructure, Mechanical Properties, Tribological

1. Introduction

The use of wear resistant castings or hard metal component in cement milling whether wet or dry mill is a well-accepted principle and the potential cost savings that will accrue by much improved wear resistant over ordinary forged white iron parts are realized in application all over the world [1] [2]. Majority of the internal wear components of a ball mill are subjected to high impact wear. This development places a high premium on the property required of such parts. Such wear part may be required to have maximum wear resistance at a level of toughness considered adequate to withstand impact forces involved [3]. Usually manufacturers of wear resistant castings are required to provide a level of assurance of freedom from premature failure since the replacement of such parts and repair can result into lost production and unscheduled shutdown time. Thus there is a need to compromise between two conflicting properties namely hardness and toughness which is a precondition for castings suitable for use in dry milling of hard solid minerals. The type of wear process in a ball mill can be classified as high abrasion and this will require an alloy that is high in chromium and carbon. It is interesting to note that 13% chromium irons that are suitable for wear resisting applications fall within the compositional limits bounded by the austenitic phase field of the ternary liquidus surface of the iron, chromium, carbon equilibrium diagram. These alloys contain between 10% to 30% and the carbon 1.0% to 3.5%.

This falls within lines corresponding to Cr/C ratio of approximately 3.5 to 15.1. Solidification begins by a eutectic process and all compositions within this family of alloys. The products of the eutectic reaction are austenite and chromium rich carbides of $(FeCr_7)C_3$ type. The eutectic morphology depends on the actual composition relative to the eutectic point. In hypo eutectic, eutectic carbides solidify in the spaces between the primary austenite dendrites in the form of grain boundary lamellae [4] [5]. This structure changed completely to lamellae as the eutectic point is reached. However, in the case of hyper eutectic alloys large hexagonal primary carbides replace the primary austenite. The actual carbides volume within the microstructure depends upon both the carbon and chromium contents [6]. In all cases the microstructure at room temperature consists of eutectic or primary carbides and austenite or one of its decomposition products.

The retained austenite in the irons is stable only at relatively high temperatures and under equilibrium conditions is prone to transform to an aggregate of very fine carbides in a matrix of ferrite [7]. The transformation product is called granular pearlite and is normally undesirable phase due to its very poor wear resistance [7]. There are two basic alternatives for the elimination of pearlitic structures which usually result to severe spalling. The first involves the prevention of pearlite formation by retaining austenite to room temperature and the second is to heat treat to produce martensitic matrix [8]. The wear behaviour was analysed as a function of applied load in the range of 50 - 250 N on titanium additions to 16% chromium white iron under pure sliding and the results revealed that the precipitated small hard titanium carbides in the proeutectic austenite promoting the strengthening of the matrix and thereby increased the bulk hardness of the alloy [5]. Effects of the ratio of C/Si, pig iron nodulariser and alloying method on the microstructure and mechanical properties of the heavy section cast (ductile) iron have been analysed and the result showed that antimony played an important role in the control of graphite morphology [9]. A novel process in semi-solid metal casting for processing casting iron was developed and the result revealed that the semi-solid metal casting effectively changed the dendritic structure of the as-cast metal to the globular ones [10]. The increase in the carbon content of high-chromium cast irons causes a decrease in the heat resistance and an increase in the rate of cracks propagation [11]. This work is aimed at studying the effects of increasing graphite additions and thermal treatment (water quenching) on the microstructure, mechanical properties such as hardness, impact energy and wear resistance of 13% chromium white iron.

2. Material and Methodology

2.1. Materials

The charge makeup used in this work were sourced from Nigerian Foundry Limited Ilupeju Lagos state Nigeria.

Two wooden patterns of $11 \times 11 \times 200$ mm were used to produce five green sand moulds from a mixture of dried fresh silica sand, bentonite, water and boiled starch with a cope and drag moulding boxes in accordance with BS 14 standard.

2.2. Methodology

A charge makeup containing foundry returns, white iron scrap and cast irons was melted in a 500 kg capacity neutral lined electric induction furnace. A weighted sample of fine graphite granules corresponding to 1.36 wt% was added to the melt at 1540°C and the temperature was maintained constant for 15 minutes to allow the graphite to dissolve after which it was poured into the mould. 1 kg of aluminium briquette was added to the melt before pouring to reduce the tendency of oxidation reaction. The solidified product of the melt represented the first batch of the 13% chromium white iron. The procedure was repeated for additional four batches with increasing wt% of graphite additions equivalent to 1.56%, 2.01%, 2.56% and 3.04% composition of the respective alloys. The elemental composition was carried out on the raw materials and the produced 13% chromium white iron with the aids of Hilger Analytical Direct Optical spectrometer, model E980C. $10 \times 10 \times 60$ mm rectangular bars were prepared from the as-cast 13% chromium white iron with the aids of Adcock Shipley Milling Machine, Model 2E.

Some of the 13% chromium white iron bars were austenised at 1450°C ; held at the temperature for 30 minutes and finally quenched in water to room temperature. The count scores, orientation and the chemical formula of phases present in the matrix of the 13% chromium white iron containing 1.36% graphite granules were determined with the aids of X-ray diffractometer. The microstructural analysis was carried out on both the as-cast and heat treated rectangular bars of the 13% chromium white iron containing 1.36% graphite granule with the aids of Scanning Electron Microscope model EVOMA 10 LaB6 Analytical VP-SEM at 20 KV.

The hardness values both of as-cast and heat treated rectangular bars of the 13% chromium white iron were determined with the aids of Brinell Hardness Tester (Dynamic Hardness Tester by Fasne Test Equipment), Model: DHT-6. The test was carried out at four different points on the surface of the samples and the average reading was recorded.

The tribological behaviour of the as-cast and heat treated rectangular bars of 13% chromium white iron containing 1.36 and 2.01 wt% graphite granules were studied with the aids of pin on disc machine. The wear test was carried out on a 200 mm circular rotating disc with attached emery paper of 180 grit size. The initial weight of the coupon before the test was measured with the aids of the digital electronic scale. The surface of the test sample was placed against the rotating disc for a period of 60 s under different applied loads and speed. The weight difference before and after the wear test were measured in grammes with the aids of digital electronic scale. The same procedure was repeated on the same wear sample at increasing cycle time from 60 to 300 s at interval of 60 s, keeping the applied load and speed constant and volume loss was calculated in each case using Equation (1).

The same procedures were repeated for the remaining samples.

$$\text{Weight loss } (w_l) = \text{initial weight} - \text{final weight} \quad (1)$$

The volume loss for each sample of experiments was calculated using Equation (2)

$$\text{Volume loss} = \frac{w_l}{\rho} \quad (2)$$

The same processes were repeated on the same wear sample under increasing applied loads (10N, 12N, 14N, 16N) and corresponding volume losses were calculated in each case. The processes were repeated on the sample under the same applied loads but higher speed ($4.72 \text{ m}\cdot\text{s}^{-1}$) of disc rotation. All the process were repeated on the respective wear sample for 1.36 and 2.01 graphite 13% chromium white iron both for as-cast and heat treated sample. The sliding distance and sliding moments were calculated using Equations (3) and (4) respectively.

$$\text{Sliding distance} = \text{sliding speed} \times \text{time} \quad (3)$$

$$\text{Sliding moment} = \text{applied load} \times \text{sliding distance} \quad (4)$$

Table 3. Identified phases and their chemical formula.

Compound name	Chromium	Chromium iron	Carbon	Martensite	Silicon	Phosphorus	Cementite
Chemical formula	Cr	Cr _{1.36} Fe _{0.52}	C	∞	Si	P	Fe ₃ C
Score	60	31	27	28	22	18	15

3.3. Microstructural Analysis

The microstructures EDS of the as-cast 1.36% graphite 13% chromium white iron is shown in **Figure 2**. It shows a typical as-cast structure that is predominantly dendritic in nature. The intermetallic compounds (iron carbide and iron chromide due to the 13% chromium content (13.12% Cr)) highly clustering at the grain boundaries influence negatively the mechanical and wear properties of the as-cast sample. Furthermore, the microstructure is fairly homogenous due to iron chromium particles that distribute almost evenly throughout the entire matrix. **Figure 3** on the other hand, shows the SEM micrograph of the heat treated sample of 1.36% graphite 13% chromium white iron. The microstructure is more homogenous than that of as-cast sample. The carbide and chromide particles are more evenly distributed within the martensitic matrix of the heat treated sample. Martensite is a non-equilibrium phase and is characterised with high hardness values. Its presence as the matrix of the heat treated sample is attributable to higher hardness values and higher wear resistance of the heat treated sample of the 1.36% graphite 13% chromium white iron.

3.4. Hardness Values

Figure 4 shows the hardness values of the as-cast and heat treated samples of the 13% chromium white iron with %composition of graphite addition. It was observed that the hardness values of the both the as-cast and heat treated samples increased as the %composition of graphite addition increased. However, increase in hardness values is due to the formation of hard intermetallic compounds. Moreover, the higher hardness values of the heat treated samples than those of the as-cast samples is attributable to presence of fine grainmartensitic matrix of the heat treated samples coupled with finely and evenly distributed chromides within the matrix as the iron chromide is known to be a very hard materials and low impact energy value.

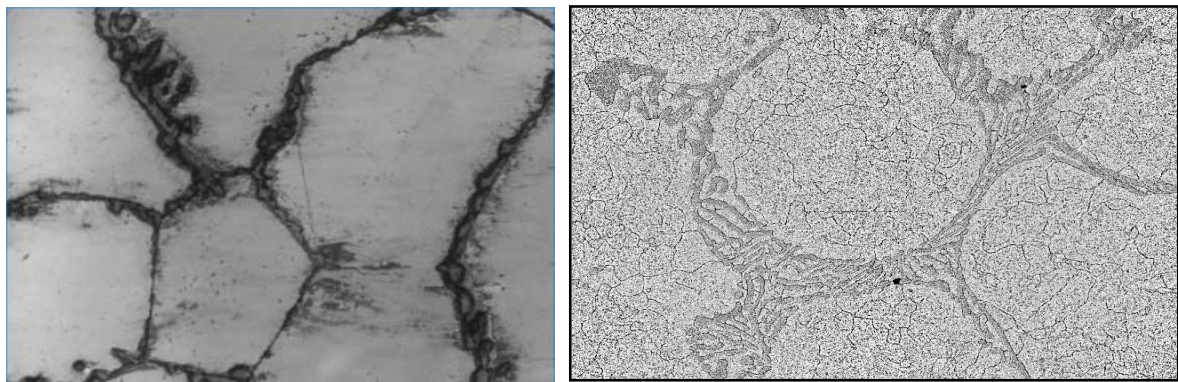
3.5. Impact Energy Values

Figure 5 shows the relationship between impact energy values of the 13% chromium white iron with %composition of graphite additions. It was observed that the impact energy values of the 13% chromium white iron decreased as %composition of graphite granule additions increased. The decrease in impact energy values is attributable to presence of graphite phase which is characterized with brittleness. Furthermore, the impact values of the heat treated sample are lower than those of the as-cast samples. The decrease in impact energy values is due to presence of very hard intermetallic cementite; very fine and hard iron chromide and hard martensitic matrix which are all characterized with small impact energy values.

3.6. Wear

Figures 6-13 show the relationship between volume loss and time when the 1.36 and 2.01 graphite samples of both the as-cast and heat treated 13% chromium white iron were subjected to wear through pin on disc method. Generally, it was observed that the volume loss during wear increased as the applied load and time of disc rotation increased. The increase in volume due to the increased surface wear of the examined sample is attributable to the increase in the work done by the friction to resist the disc rotation. Furthermore, the MATLAB linear fitting approach was applied to each line in **Figures 6-13** to generate the volume loss equations (see Equations (5)-(44)). The wear rate in cubic meter per second at each applied load was obtained as a gradient of each equation for both the as-cast and heat treated 13% chromium white iron (see **Table 4** and **Table 5**).

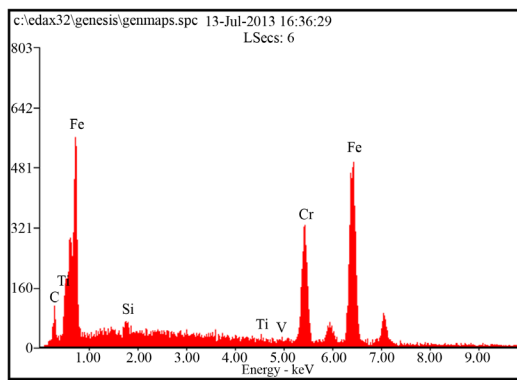
Similarly, **Figure 14** and **Figure 15** show the relationship between sliding moments and time at 2.36 and 4.72 m·s⁻¹. It was observed the sliding moments increased as the time of contact of the wear sample and emery paper increased under load applications. Also, the sliding moments increased with speed. The sliding moment per second was obtained both for low and high speed from the gradient of the linear sliding moment equations (see Equations (45)-(54) and **Table 4** and **Table 5**).



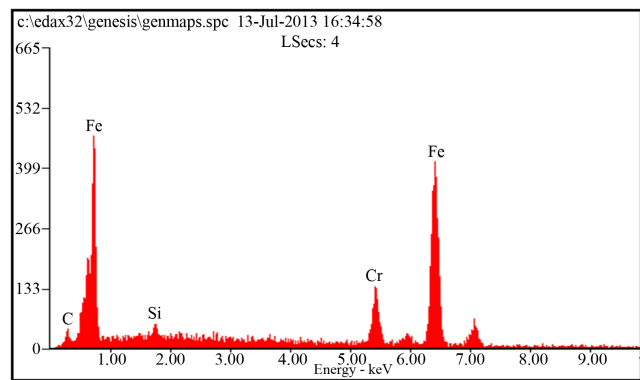
(a)

(b)

Figures 2. SEM micrographs & EDS of the as-cast 1.36% graphite 13% chromium white iron.



(a)



(b)

Figures 3. SEM micrographs & EDS of the heat treated 1.36% graphite 13% chromium white iron.

Table 4. Wear parameters of 1.36% graphite 13% chromium white iron.

Load N	Sliding moment/second $N \cdot m \cdot s^{-1}$ at $2.36 \text{ m} \cdot s^{-1}$	Sliding moment/second $N \cdot m \cdot s^{-1}$ at $4.72 \text{ m} \cdot s^{-1}$	As-cast		Heat treated	
			Wear rate $m^3 \cdot s^{-1}$ at $2.36 \text{ m} \cdot s^{-1} \times 10^{-10}$	Wear rate $m^3 \cdot s^{-1}$ at $4.72 \text{ m} \cdot s^{-1} \times 10^{-10}$	Wear rate $m^3 \cdot s^{-1}$ at $2.36 \text{ m} \cdot s^{-1} \times 10^{-10}$	Wear rate $m^3 \cdot s^{-1}$ at $4.72 \text{ m} \cdot s^{-1} \times 10^{-10}$
6	14.16	28.32	2.838	5.143	1.703	3.043
10	23.60	47.2	3.400	6.400	1.999	3.838
12	28.29	56.58	5.043	11.100	3.022	6.665
14	33.04	66.08	6.067	12.570	3.639	7.663
16	37.76	75.52	6.838	13.540	4.095	8.071

Table 5. Wear parameters of 2.01% graphite 13% chromium white iron.

Load N	Sliding moment/second $N \cdot m \cdot s^{-1}$ at $2.36 \text{ m} \cdot s^{-1}$	Sliding moment/second $N \cdot m \cdot s^{-1}$ at $4.72 \text{ m} \cdot s^{-1}$	As-cast		Heat treated	
			Wear rate $m^3 \cdot s^{-1}$ at $2.36 \text{ m} \cdot s^{-1} \times 10^{-10}$	Wear rate $m^3 \cdot s^{-1}$ at $4.72 \text{ m} \cdot s^{-1} \times 10^{-10}$	Wear rate $m^3 \cdot s^{-1}$ at $2.36 \text{ m} \cdot s^{-1} \times 10^{-10}$	Wear rate $m^3 \cdot s^{-1}$ at $4.72 \text{ m} \cdot s^{-1} \times 10^{-10}$
6	14.16	28.32	2.122	3.861	1.443	2.612
10	23.60	47.2	2.644	4.872	1.729	3.313
12	28.29	56.58	3.785	8.352	2.575	5.682
14	33.04	66.08	4.572	9.429	3.157	6.430
16	37.76	75.52	5.148	11.960	3.501	8.135

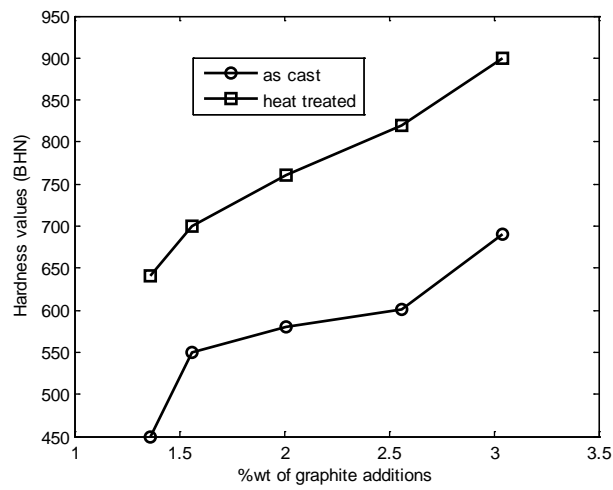


Figure 4. Hardness values wt% of graphite additions.

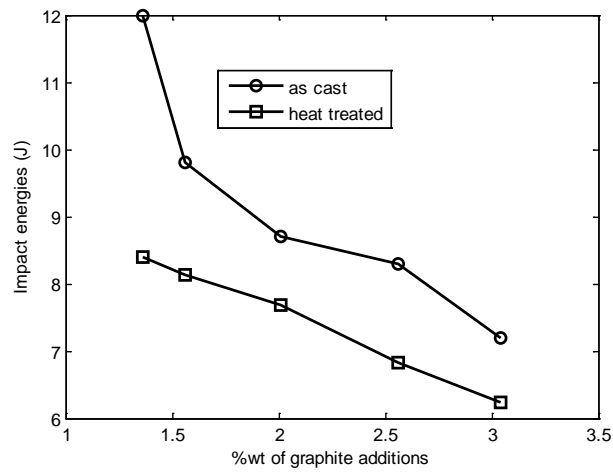


Figure 5. Impact energy values with wt% of graphite additions.

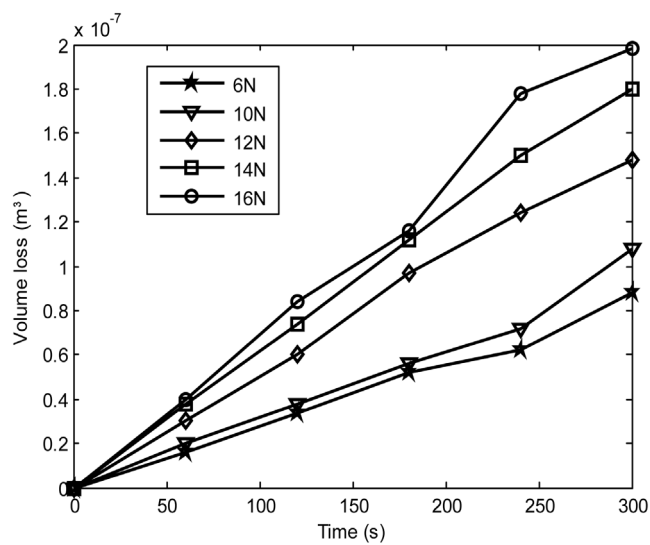


Figure 6. Volume loss with time of the as-cast 1.36% graphite 13% chromium white iron at $2.36 \text{ m}\cdot\text{s}^{-1}$.

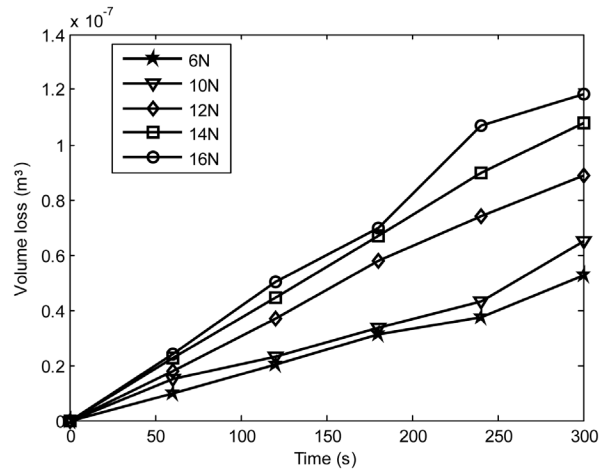


Figure 7. Volume loss with time of the 1.36% graphite of the heat treated 13% chromium white iron at $2.36 \text{ m}\cdot\text{s}^{-1}$.

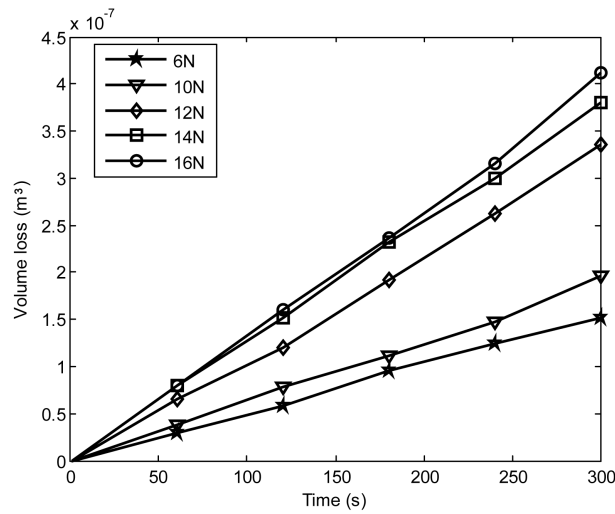


Figure 8. Volume loss with time of the as-cast 1.36% graphite 13% chromium white iron at $4.72 \text{ m}\cdot\text{s}^{-1}$.

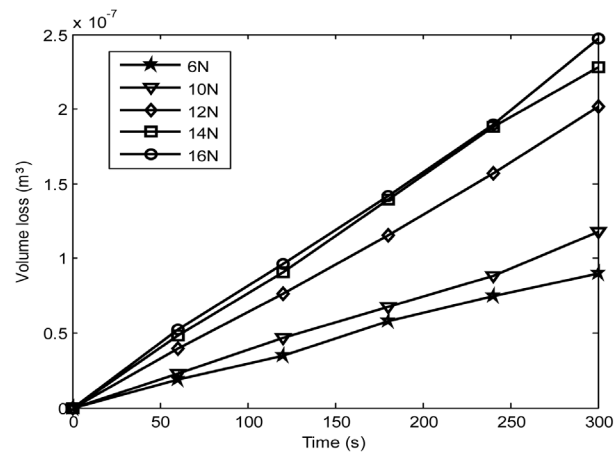


Figure 9. Volume loss with time of the heat treated 1.36% graphite 13% chromium white iron at $4.72 \text{ m}\cdot\text{s}^{-1}$.

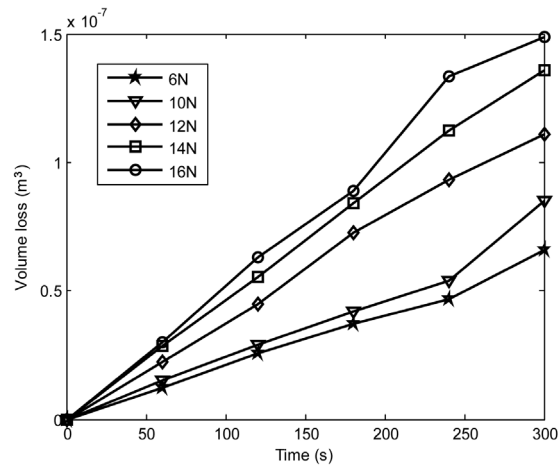


Figure 10. Volume loss with time of the as-cast 2.01% graphite 13% chromium white iron at $2.36 \text{ m}\cdot\text{s}^{-1}$.

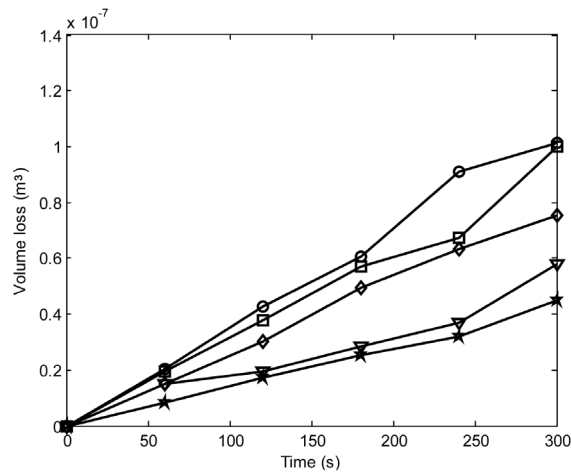


Figure 11. Volume loss with time of the heat treated 2.01% graphite 13% chromium white iron at $2.36 \text{ m}\cdot\text{s}^{-1}$.

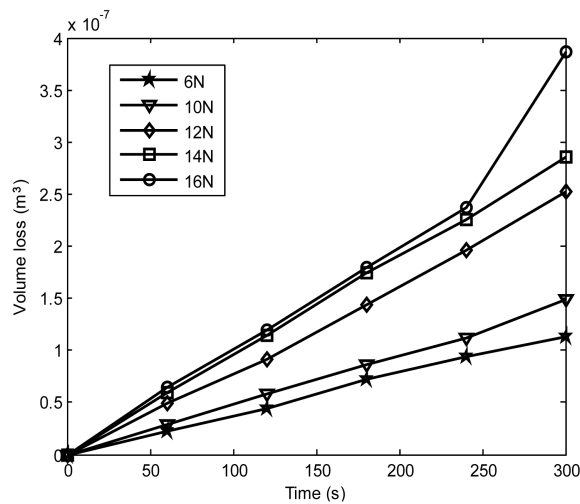


Figure 12. Volume loss with time of the as-cast 2.01% graphite 13% chromium white iron at $4.72 \text{ m}\cdot\text{s}^{-1}$.

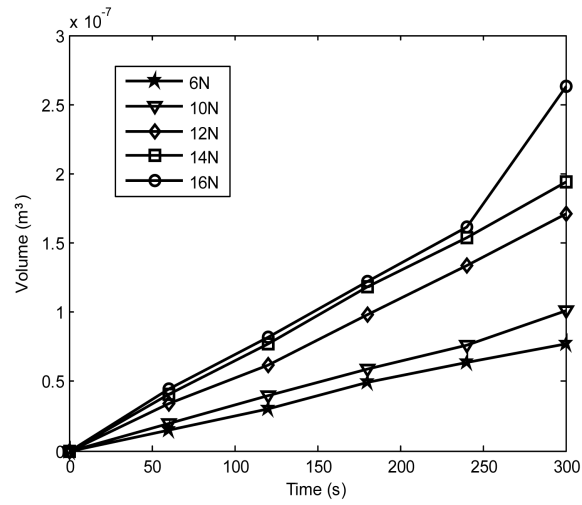


Figure 13. Volume loss with time of the heat treated 2.01% graphite 13% chromium white iron at $4.72 \text{ m}\cdot\text{s}^{-1}$.

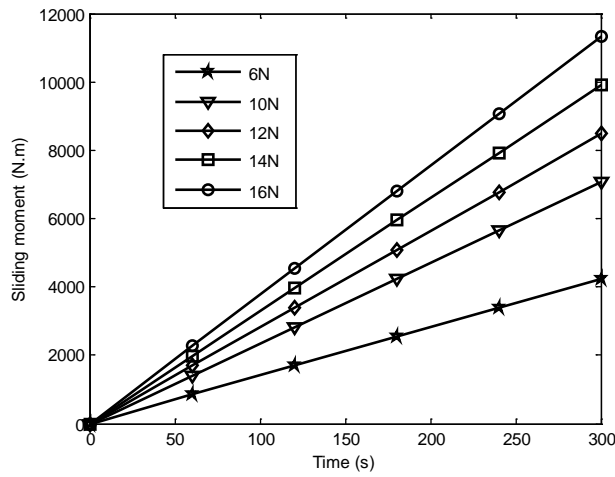


Figure 14. Sliding moment with time at $2.36 \text{ m}\cdot\text{s}^{-1}$.

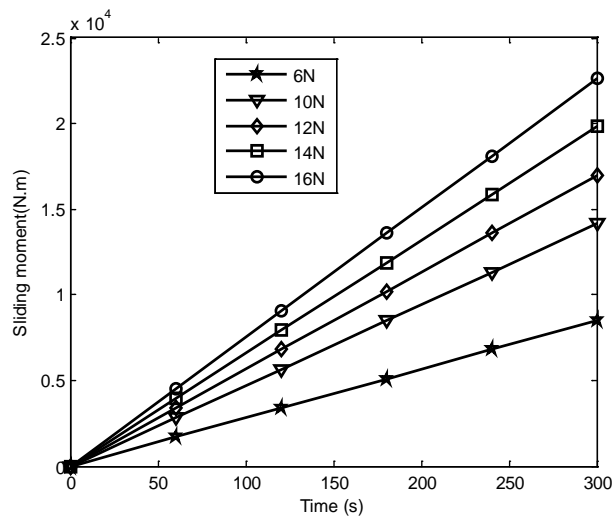


Figure 15. Sliding moment with time at $4.726 \text{ m}\cdot\text{s}^{-1}$.

3.6.1. Volume Loss Equations for 13% Chromium White Iron

1) 1.36% graphite sample (as-cast) at $2.36 \text{ m}\cdot\text{s}^{-1}$

$$y_{6N} = 2.838 \times 10^{-10} x - 5.714 \times 10^{-10} \quad (5)$$

$$y_{10N} = 3.4 \times 10^{-10} x - 2 \times 10^{-9} \quad (6)$$

$$y_{12N} = 5.043 \times 10^{-10} x - 2 \times 10^{-10} \quad (7)$$

$$y_{14N} = 6.067 \times 10^{-10} x + 1.333 \times 10^{-9} \quad (8)$$

$$y_{16N} = 6.838 \times 10^{-10} x - 9.524 \times 10^{-11} \quad (9)$$

2) 1.36% graphite sample (heat treated) at $2.36 \text{ m}\cdot\text{s}^{-1}$

$$y_{6N} = 1.703 \times 10^{-10} x - 3.429 \times 10^{-10} \quad (10)$$

$$y_{10N} = 1.999 \times 10^{-10} x - 5.238 \times 10^{-11} \quad (11)$$

$$y_{12N} = 3.022 \times 10^{-10} x + 7.048 \times 10^{-10} \quad (12)$$

$$y_{14N} = 3.639 \times 10^{-10} x - 7.81 \times 10^{-10} \quad (13)$$

$$y_{16N} = 4.095 \times 10^{-10} x - 1.381 \times 10^{-10} \quad (14)$$

3) 1.36% graphite sample (as-cast) at $4.72 \text{ m}\cdot\text{s}^{-1}$

$$y_{6N} = 5.143 \times 10^{-10} x - 4.762 \times 10^{-10} \quad (15)$$

$$y_{10N} = 6.4 \times 10^{-10} x - 6.667 \times 10^{-10} \quad (16)$$

$$y_{12N} = 1.114 \times 10^{-9} x - 4.476 \times 10^{-9} \quad (17)$$

$$y_{14N} = 1.257 \times 10^{-9} x - 2.095 \times 10^{-9} \quad (18)$$

$$y_{16N} = 1.354 \times 10^{-9} x - 2.476 \times 10^{-9} \quad (19)$$

4) 1.36% graphite sample (heat treated) at $4.27 \text{ m}\cdot\text{s}^{-1}$

$$y_{6N} = 3.043 \times 10^{-10} x - 3.667 \times 10^{-10} \quad (20)$$

$$y_{10N} = 3.838 \times 10^{-10} x - 4.476 \times 10^{-10} \quad (21)$$

$$y_{12N} = 6.665 \times 10^{-10} x - 1.705 \times 10^{-9} \quad (22)$$

$$y_{14N} = 7.663 \times 10^{-10} x - 7.905 \times 10^{-10} \quad (23)$$

$$y_{16N} = 8.071 \times 10^{-10} x - 4.762 \times 10^{-12} \quad (24)$$

5) 2.01% graphite sample (as-cast) at $2.36 \text{ m}\cdot\text{s}^{-1}$

$$y_{6N} = 2.122 \times 10^{-10} x - 6.286 \times 10^{-10} \quad (25)$$

$$y_{10N} = 2.664 \times 10^{-10} x - 2.19 \times 10^{-9} \quad (26)$$

$$y_{12N} = 3.785 \times 10^{-10} x - 5.619 \times 10^{-10} \quad (27)$$

$$y_{14N} = 4.572 \times 10^{-10} x - 8.476 \times 10^{-10} \quad (28)$$

$$y_{6N} = 5.148 \times 10^{-10} x + 1.952 \times 10^{-10} \quad (29)$$

6) 2.01% graphite sample (heat treated) at $2.36 \text{ m}\cdot\text{s}^{-1}$

$$y_{6N} = 1.443 \times 10^{-10} x - 4.276 \times 10^{-10} \quad (30)$$

$$y_{10N} = 1.729 \times 10^{-10} x + 3.667 \times 10^{-10} \quad (31)$$

$$y_{12N} = 2.575 \times 10^{-10} x - 3.19 \times 10^{-10} \quad (32)$$

$$y_{14N} = 3.157 \times 10^{-10} x - 4.586 \times 10^{-10} \quad (33)$$

$$y_{16N} = 3.501 \times 10^{-10} x - 1.186 \times 10^{-10} \quad (34)$$

7) 2.01% graphite sample (as-cast) at $4.72 \text{ m}\cdot\text{s}^{-1}$

$$y_{6N} = 3.86 \times 10^{-10} x - 3.048 \times 10^{-10} \quad (35)$$

$$y_{10N} = 4.872 \times 10^{-10} x - 7.524 \times 10^{-10} \quad (36)$$

$$y_{12N} = 8.352 \times 10^{-10} x - 3.129 \times 10^{-9} \quad (37)$$

$$y_{14N} = 9.429 \times 10^{-10} x - 1.571 \times 10^{-9} \quad (38)$$

$$y_{16N} = 11.96 \times 10^{-9} x - 1.452 \times 10^{-8} \quad (39)$$

8) 2.01% graphite sample (heat treated) at $4.27 \text{ m}\cdot\text{s}^{-1}$

$$y_{6N} = 2.612 \times 10^{-10} x - 1.843 \times 10^{-10} \quad (40)$$

$$y_{10N} = 3.313 \times 10^{-10} x - 5.076 \times 10^{-10} \quad (41)$$

$$y_{12N} = 5.682 \times 10^{-10} x - 2.146 \times 10^{-9} \quad (42)$$

$$y_{14N} = 6.43 \times 10^{-10} x - 8.976 \times 10^{-10} \quad (43)$$

$$y_{16N} = 8.135 \times 10^{-10} x - 9.878 \times 10^{-9} \quad (44)$$

9) Sliding moment equations

$$y_{6N} = 14.16x + 9.524 \times 10^{-2} \quad (45)$$

$$y_{10N} = 23.6x - 1.316 \times 10^{-22} \quad (46)$$

$$y_{12N} = 28.29x + 9.524 \times 10^{-2} \quad (47)$$

$$y_{14N} = 33.04x + 2.222 \times 10^{-12} \quad (48)$$

$$y_{16N} = 37.76x + 2.55 \times 10^{-12} \quad (49)$$

$$y_{6N} = 28.32x + 1.429 \times 10^{-2} \quad (50)$$

$$y_{10N} = 47.2x + 2.633 \times 10^{-12} \quad (51)$$

$$y_{12N} = 56.64x + 9.524 \times 10^{-2} \quad (52)$$

$$y_{14N} = 66.08x + 2.381 \times 10^{-2} \quad (53)$$

$$y_{16N} = 75.51x + 5.238 \times 10^{-2} \quad (54)$$

Figure 16 and **Figure 17** show the relationship between wear rate and sliding moment per unit time of both the as-cast and heat treated samples of 13% chromium white iron at 2.36 and $4.72 \text{ m}\cdot\text{s}^{-1}$ respectively. It was observed that the wear rate increased as the sliding moment per unit time increased. The MATLAB linear fitting approach was applied to generate the wear rate equations (see Equations (55)-(62)). The wear coefficient which is the gradient of the wear rate-sliding moment per unit time graph was obtained from each equation using the first differential approach (see **Table 6**). The wear resistance of both the as-cast and heat treated samples of 13% chromium white iron was calculated as the reciprocal of wear coefficients. In order to investigate the effect of speed increase and %composition of graphite additions on the wear resistance of the 13% chromium white iron,

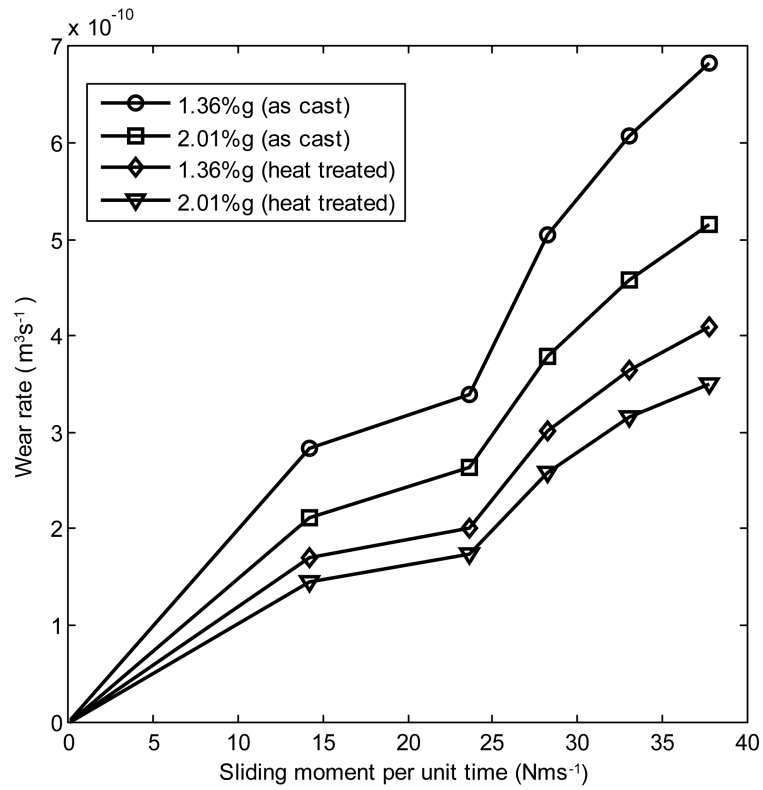


Figure 16. Wear rate of 13% chromium white iron with sliding moment per unit time at $2.36 \text{ m}\cdot\text{s}^{-1}$.

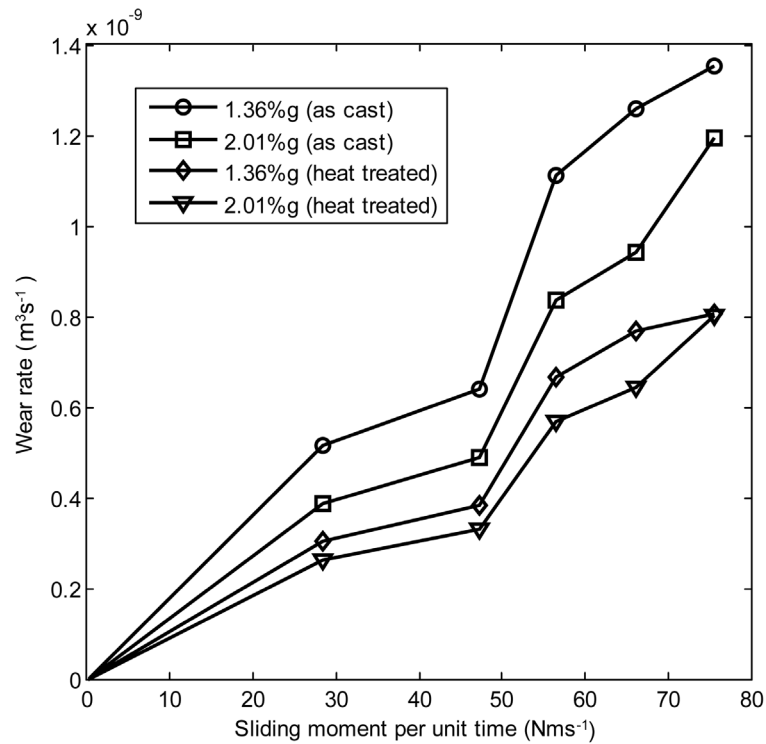


Figure 17. Wear rate of 13% chromium white iron with sliding moment per unit time at $4.72 \text{ m}\cdot\text{s}^{-1}$.

Table 6. Wear parameters of 1.36% graphite 13% chromium white iron.

wt% of graphite addition	Samples	Wear coefficient at $2.36 \text{ m}\cdot\text{s}^{-1}\cdot\text{N}\cdot\text{m}^{-2} \times 10^{-11}$	Wear resistance at $2.36 \text{ m}\cdot\text{s}^{-1}\cdot\text{N}\cdot\text{m}^{-2} \times 10^{10}$	Wear coefficient at $4.72 \text{ m}\cdot\text{s}^{-1}\cdot\text{N}\cdot\text{m}^{-2} \times 10^{-11}$	Wear resistance at $4.72 \text{ m}\cdot\text{s}^{-1}\cdot\text{N}\cdot\text{m}^{-2} \times 10^{10}$
1.36	As-cast	1.783	5.6085	1.848	5.4113
1.36	Heat treated	1.068	9.3633	1.113	8.9847
2.01	As-cast	1.344	7.440	1.528	6.5445
2.01	Heat treated	0.9188	10.8838	1.031	9.6993

the graph of wear resistances of both the as-cast and heat treated samples of the produced 13% chromium white iron was plotted with speed and %composition of graphite additions respectively (see **Figure 18** and **Figure 19**). **Figure 18** reveals that the wear resistances of the heat treated samples of 13% chromium white iron containing 1.36% and 2.01% graphite slightly decreased as the speed of the pin on disc increased whereas in the case of as-cast samples, the wear resistances are almost unchanged as the speed increased. However, the speed increase has much small effects on the wear resistance of both the as-cast and heat treated samples of 13% chromium white iron but its effect on decreasing wear resistances was more pronounced on heat treated samples than on the as-cast samples though the wear resistances of the heat treated samples are much greater than that of the as-cast samples. In **Figure 19**, it was observed that the wear resistances both of the as-cast and heat treated samples increased as the %composition of graphite additions increased. This is attributable to increased resistance of both samples as the %composition of graphite additions increased.

3.6.2. Wear Rate Equations at $2.36 \text{ m}\cdot\text{s}^{-1}$

$$y_{1.36\% \text{ graphite sample (as cast)}} = 1.783 \times 10^{-11} x - 3.624 \times 10^{-12} \quad (55)$$

$$y_{2.01\% \text{ graphite sample (as cast)}} = 1.344 \times 10^{-11} x - 2.104 \times 10^{-12} \quad (56)$$

$$y_{1.36\% \text{ graphite sample (heat treated)}} = 1.068 \times 10^{-11} x - 3.624 \times 10^{-12} \quad (57)$$

$$y_{2.01\% \text{ graphite sample (heat treated)}} = 9.188 \times 10^{-12} x - 2.824 \times 10^{-12} \quad (58)$$

3.6.3. Wear Rate Equations at $4.72 \text{ m}\cdot\text{s}^{-1}$

$$y_{1.36\% \text{ graphite sample (as cast)}} = 1.848 \times 10^{-11} x - 3.026 \times 10^{-12} \quad (59)$$

$$y_{2.01\% \text{ graphite sample (as cast)}} = 1.528 \times 10^{-11} x - 5.584 \times 10^{-12} \quad (60)$$

$$y_{1.36\% \text{ graphite sample (heat treated)}} = 1.113 \times 10^{-11} x - 1.97 \times 10^{-12} \quad (61)$$

$$y_{2.01\% \text{ graphite sample (heat treated)}} = 1.031 \times 10^{-12} x - 3.617 \times 10^{-11} \quad (62)$$

4. Conclusions

From the results and discussion of this work, the following findings can be drawn:

- The hardness values of the 13% chromium white iron increased with increased percentage of carbon additions. However, the impact energy values are sacrificed.
- The oil quenched 13% chromium white cast iron possesses greater hardness values than as-cast samples.
- The lower impact values of the oil quenched samples of 13% chromium white are attributable to hard martensitic phase which is very brittle
- The increased hardness along with increasing wt% of graphite additions is attributable to presence of carbide particles in the iron matrix.
- Variation of wear with respect to time increases with increasing level of load on the material as with increase in load, there will be more friction at the surfaces in contact, which leads to increase in wear of material.

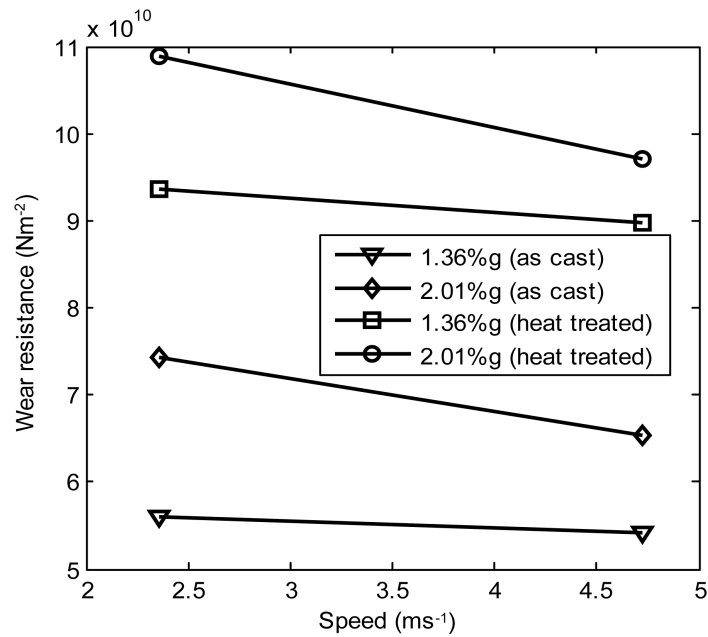


Figure 18. Wear resistance of 13% chromium white iron with speed of pin on disc.

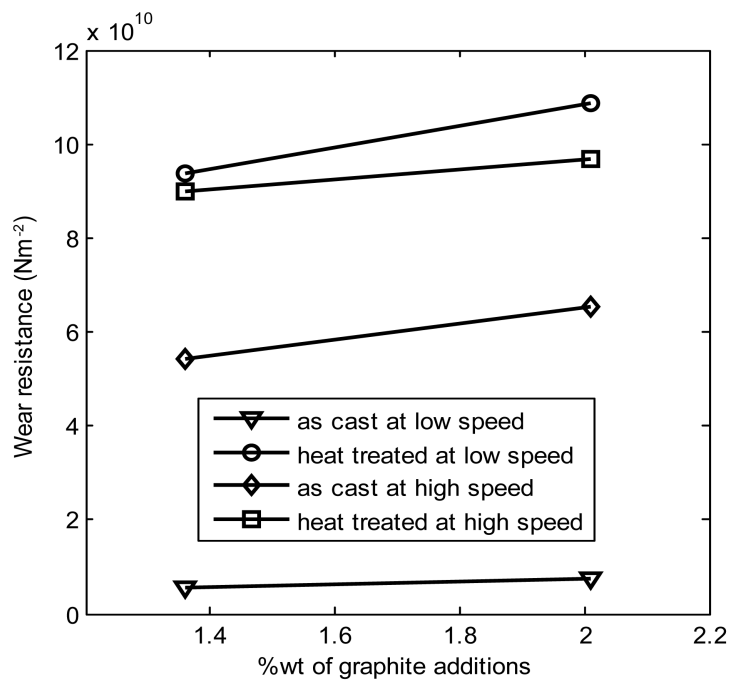


Figure 19. Wear resistance of 13% chromium white iron with wt% of graphite additions.

- This type of trend has taken place in case of annealed samples subjected to different load variations.
- The wear rate with respect to time or sliding distance for the samples in various loading conditions follows the decreasing trend.
 - Well distributed chromium carbide crystals precipitated away from the grain boundaries and the matrix of martensite produced high hardness than the as-cast. Thus quenching in oil baths after heat treatment promoted the formation of fine crystals of chromium carbide well distributed in the martensite matrix.

Acknowledgements

The authors wish to acknowledge the valuable contribution of Engr Ogundare of the Engineering Material Development Institute, Akure Ondo State Nigeria and Mr Raheem of Physics Department, University of Lagos, Akoka Lagos for their assistance in carrying out some tests.

References

- [1] Higgins, R.A. (1974) Engineering Metallurgy. Part 1. 2nd Edition, Edward Arnold, 237.
- [2] Ono, Y., Murai, N. and Ogi, K. (1992) Partition Coefficients of Alloying Elements to Primary Austenite and Eutectic Phases of Chromium Iron for Rolls. *ISIJ International*, **32**, 1150-1156. <http://dx.doi.org/10.2355/isijinternational.32.1150>
- [3] Liu, Z.L., Chen, X., Li, Y.X. and Hu, K.H. (2008) Effect of Chromium on Microstructure and Properties of High Boron White Cast Iron. *Metallurgical and Materials Transaction A*, **39**, 636-641.
- [4] Tabrett, C.P., Sare, I.R. and Ghomashchi, M.R. (1996) Microstructure-Property Relationships in 13% Chromium White Iron Alloys. *International Materials Reviews*, **41**, 52-89. <http://dx.doi.org/10.1179/imr.1996.41.2.59>
- [5] Bedolla-Jacuinde, A. and Rainforth, W.M. (2001) The Wear Behaviour of 13% Chromium White Cast Irons as a Function of Silicon and Mischmetal Content. *Wear*, **250**, 449-460. [http://dx.doi.org/10.1016/S0043-1648\(01\)00633-0](http://dx.doi.org/10.1016/S0043-1648(01)00633-0)
- [6] Zum-Gahr, K.H. and Eldis, G.T. (1980) Abrasive Wear of White Cast Irons. *Wear*, **64**, 175-194. [http://dx.doi.org/10.1016/0043-1648\(80\)90101-5](http://dx.doi.org/10.1016/0043-1648(80)90101-5)
- [7] Etinkaya, C.C. (2006) An Investigation of the Wear Behaviours of White Cast Irons under Different Compositions. *Journal Material Description*, **27**, 437-445.
- [8] Zum-Gahr, Z.H. and Scholz, W.G. (1980) Fracture Toughness of White Cast Irons. *Journal of Metallurgy*, **38**, 34-44.
- [9] Bai, Y.L., Luan, Y.K., Song, N.N., Kang, X.H., Li, D.Z. and Li, Y.Y. (2012) Chemical Composition, Microstructure and Mechanical Properties of Roll Core Used Ductile Iron in Centrifugal Casting Composite Roll. *Journal of Material Science and Technology*, **28**, 853-858. [http://dx.doi.org/10.1016/S1005-0302\(12\)60142-X](http://dx.doi.org/10.1016/S1005-0302(12)60142-X)
- [10] Abbasi-Khazaei, B. and Ghaderi, S. (2012) A Novel Process in Semi Solid Metal Casting. *Journal of Materials Science & Technology*, **28**, 946-950. [http://dx.doi.org/10.1016/S1005-0302\(12\)60156-X](http://dx.doi.org/10.1016/S1005-0302(12)60156-X)
- [11] Sun, Z.P., Zuo, R.L., Li, C., Shen, B.L., Yan, J. and Huang, S.J. (2002) TEM Study on Precipitation and Transformation of Secondary Carbides in 16Cr-1Mo-1%Cu White Iron Subjected to Subcritical Treatment. *Materials Characterization*, **53**, 403-409.

Scientific Research Publishing (SCIRP) is one of the largest Open Access journal publishers. It is currently publishing more than 200 open access, online, peer-reviewed journals covering a wide range of academic disciplines. SCIRP serves the worldwide academic communities and contributes to the progress and application of science with its publication.

Other selected journals from SCIRP are listed as below. Submit your manuscript to us via either submit@scirp.org or [Online Submission Portal](#).

